Conformational and structural determination of F2NC(O)F and F2NC(O)NCO. A joint experimental and theoretical study

ARTICLE *in* THE JOURNAL OF PHYSICAL CHEMISTRY A · OCTOBER 2009

Impact Factor: 2.69 · DOI: 10.1021/jp907827q · Source: PubMed

Conformational and Structural Determination of $F_2NC(O)F$ and $F_2NC(O)NCO$. A Joint Experimental and Theoretical Study

Mauricio F. Erben,[‡] Juan M. Padró,[‡] Helge Willner,[§] and Carlos O. Della Védova*[,‡,||]

CEQUINOR (UNLP-CONICET, CCT La Plata), Departamento de Química, Facultad de Ciencias Exactas, Universidad Nacional de La Plata, CC 962, La Plata (CP 1900), República Argentina, Fachbereich C-Anorganische Chemie, Bergische Universität Wuppertal, Gaussstrasse 20, 47097 Wuppertal, Germany, and Laboratorio de Servicios a la Industria y al Sistema Científico (LaSeISiC) (UNLP-CIC-CONICET), Camino Centenario e/505 y 508, (1903) Gonnet, República Argentina

Received: August 13, 2009; Revised Manuscript Received: September 11, 2009

The vibrational properties of two difluoroaminocarbonyl species were analyzed by recording the FTIR spectra of the vapor for difluoroaminocarbonyl fluoride, $F_2NC(O)F$, and difluoroaminocarbonyl isocyanate, $F_2NC(O)NCO$. Moreover, the Raman spectrum of liquid $F_2NC(O)NCO$ was obtained. Vibrational assignments were made on the basis of a normal coordinate analysis and the evaluation of the band contours appearing in the FTIR spectrum of the vapor. The conformational space of both difluoroaminocarbonyl derivatives were studied by using the B3LYP and MP2 level of theory with extended basis sets [6-311+G(3df) and aug-cc-pVTZ]. Only one conformation belonging to the C_1 symmetry point group is expected for $F_2NC(O)F$, whereas the overall evaluation of experimental and theoretical results suggests the existence of a mixture of two conformers for $F_2NC(O)NCO$ at room temperature. Its relative abundance of the most stable syn form (C═O double bond syn with respect to the N═C═O group) was estimated to be 56(5) %.

Introduction

Attempts to prepare difluoroaminocarbonyl fluoride, $F_2NC(O)F$, were first reported by Ruff and Giese in 1936.[1] When trifluoronitrosomethane, CF_3NO, contacts aqueous sodium hydroxide, nearly quantitative conversion to its isomer [$F_2NC(O)F$] occurs.[2] However, some controversies appeared when Haszeldine and Jander concluded that the earlier reported compound was either perfluoroethane (C_2F_6) or perfluoromethylamine (CF_3NF_2) and, therefore, that $F_2NC(O)F$ was elusive so far.[3] Finally, in 1965 Fraser et al.[4] synthesized $F_2NC(O)F$ through ultraviolet irradiation of a mixture of tetrafluorohydrazine and carbon monoxide. The chemistry of $F_2NC(O)F$ was further extended by the same authors.[5] Subsequently, pseudohalide derivatives $NF_2C(O)X$ (X = CN, NCO, NCS, and SCF_3) were prepared by reacting $F_2NC(O)Cl$ with silver or mercury salts.[6]

The synthetic interest in difluoramines attracted considerable attention, including the preparation of poly(difluoroamino)alkanes, difluoroaminoalkanols, and diazirines from aldehydes, ketones, alkynes, alkenes, ethers, and imines.[7] Difluoramines are also good candidates as energetic materials in rocket propellant and explosives formulations. This chemical potential derives from the intrinsically high energy of the difluoroamino ($-NF_2$) group relative to other substituents of oxidizing capability in energetic ingredients, such as the nitro group (NO_2).[8]

As a part of our general project concerning structural and vibroconformational properties of covalent molecular species, we became interested in two difluoraminocarbonyl molecules, namely, $F_2NC(O)F$ and $F_2NC(O)NCO$.

In particular, the conformational composition of simple isocyanates has been difficult to predict and may also vary in different aggregation states. For example, acetyl isocyanate, $CH_3C(O)NCO$,[9] shows dramatic conformational changes when the compound is measured in the gas or in the liquid phase. Furthermore, the conformational stability of XC(O)NCO (X = F[10,11] Cl,[12–14] Br,[15] CH_3,[9,16,17] and CF_3[10]) molecules in the vapor state depends on the X substituent. Some controversy has been also reported over the experimental and the calculated conformational properties of simple isocyanates, challenging the reliability of ab initio calculations. For instance, while the vibrational spectra[12,13] and gas electron diffraction studies for ClC(O)NCO[14] in both the gas and liquid phases are consistent with the preference of the anti form (the isocyanate group anti with respect to the C═O double bond), most ab initio calculations predict the syn form as the most stable conformer.[14,18–20] On the other hand, the conformational properties of acetyl isocyanate derivatives RC(O)NCO (R = CH_xCl_{3-x}[21–24]) and CH_2═CHC(O)NCO[25] have been reported recently, resulting in a preferred syn conformation in the gas phase.

In this work, infrared measurements of gaseous difluoraminocarbonyl fluoride, $F_2NC(O)F$, and difluoraminocarbonyl isocyanate, $F_2NC(O)NCO$, as well as extensive quantum chemical calculations were made. The Raman spectrum of liquid $F_2NC(O)NCO$ was also obtained. Thus, the vibrational and structural properties were determined for both molecules.

Experimental Section

Caution! Nitrogen−fluorine-containing materials are strongly oxidizing. Handling and freezing of such materials must always be done with adequate precautions. The materials are potentially hazardous and proper shielding should be used.

Synthesis. $NF_2C(O)F$ was synthesized by irradiation of a mixture of N_2F_4 and carbon monoxide according to the method reported by Fraser and Shreeve.[4] $F_2NC(O)NCO$ was obtained by reacting $NF_2C(O)F$ with excess of dry AgNCO following the method reported elsewhere.[6] Both compounds were purified

* To whom correspondence should be addressed. Tel/Fax ++54-221-425-9485. E-mail:carlosdv@quimica.unlp.edu.ar.
‡ Universidad Nacional de La Plata.
§ Bergische Universität Wuppertal.
|| Laboratorio de Servicios a la Industria y al Sistema Científico.

10.1021/jp907827q CCC: $40.75
Published on Web 10/07/2009

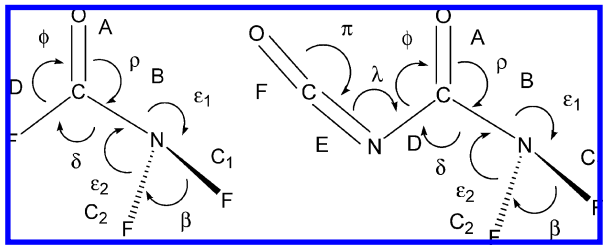

Figure 1. Internal coordinates for $F_2NC(O)X$ (X = F and NCO) compounds.

by trap-to-trap distillation and the final purity was checked by IR and ^{19}F NMR spectroscopy.

General Procedure. Volatile materials were manipulated in a glass vacuum line equipped with two capacitance pressure gauges (221 AHS-1000 and 221 AHS-10, MKS Baratron, Burlington, MA), three U-traps, and valves with PTFE stems (Young, London, UK). The vacuum line was connected to an IR cell (optical path length 200 mm, Si windows 0.5 mm thick) contained in the sample compartment of an FTIR instrument (Impact 400D, Nicolet, Madison, WI). This allowed us to monitor the purification processes and to follow the course of the reactions. Pure compounds were stored in flame-sealed glass ampules under liquid nitrogen in a long-term Dewar vessel. The ampules were opened with an ampule key on the vacuum line, an appropriate amount of the compound was taken out for the experiments, and then the ampules were flame-sealed again.[26]

Vibrational Spectroscopy. Gas-phase infrared spectra were recorded with a resolution of 1 cm^{-1} in the range 4000−400 cm^{-1} with a Bruker IFS 66v FTIR instrument and Raman spectra of liquid with a Bruker RFS 100/S FT-Raman spectrometer. The liquid sample of $F_2NC(O)NCO$ was contained in a 4 mm glass capillary and the spectrum excited with 500 mW of 1064 nm radiation from a Nd:YAG laser (ADLAS, DPY 301, Lübeck, Germany).

Computational Methods. All quantum chemical calculations were performed with the Gaussian 03 program package.[27] MP2 and B3LYP methods and gradient techniques were used for the geometry optimizations and calculation of the vibrational properties, together with standard basis sets up to the Pople-type 6-311+G(3df) and the augmented Dunning's correlation-consistent basis sets of valence triple-ζ (aug-cc-pVTZ). The 6-311+G(3df) basis set includes diffuse and polarization functions and has been shown to be near the basis set saturation limit when used with the B3LYP functional.[28] For $F_2NC(O)F$, higher-order electron correlation effects were explicitly included in the geometry optimization by using the CCSD(T)/6-311+G* level of approximation. Transition states were optimized by the synchronous transit-guided quasi-Newton (STQN) method, and torsional barrier heights were calculated from the relative energies of the TS and the stable structure with the zero-point energies of the species taken into account. All computed TS structures show only one imaginary frequency, which corresponds to the torsion involved in the conformational transition. For the normal coordinate analysis, transformations of the ab initio Cartesian harmonic force constants to the molecule-fixed internal coordinates system were performed, as described by Hedberg and Mills and implemented in the ASYM40 program.[29] This procedure evaluates the potential energy distribution (PED) associated with each normal vibrational mode under the harmonic assumption. The internal and symmetry coordinates used to perform the normal coordinate analysis are defined in Figure 1 and Table 1, respectively.

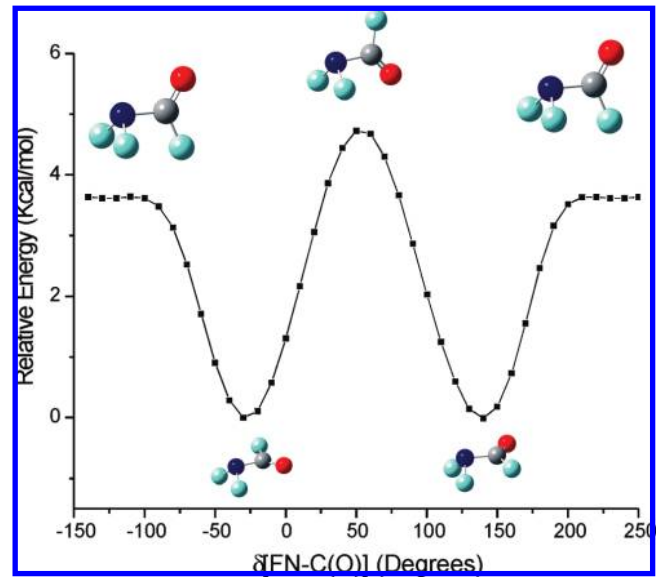

Figure 2. Calculated potential function (B3LYP/6-311+G*) for the internal rotation around the N−C bond in $F_2NC(O)F$.

Results and Discussion

Conformational Space and Molecular Structure of $F_2NC(O)F$. The potential function for the internal rotation around the central N−C bond was derived by structure optimizations at fixed δ[FN−C(O)] dihedral angles. The potential function obtained from the B3LYP/6-311+G* method is shown in Figure 2. The curve is symmetrical with respect to a global maximum located at δ[FN−C(O)] = 60°, with equivalent minima at dihedral angles at around 140° and −30°, corresponding to two nonplanar enantiomeric forms. Both minima are connected through torsional transition states with δ[FN−C(O)] = 60° and 250° (or −140°), with barriers for internal rotation of 4.8 and 3.8 kcal/mol, respectively. These transition states present C_S symmetry, with the FC(O) group bisecting the NF_2 plane. The transition state structure with a δ[FN−C(O)] value of ca. 250° is located in a flat portion of the potential curve.

The molecular structure for the minimum was fully optimized by using several levels of theoretical approximations, including the B3LYP method with the 6-311+G(3df) and aug-cc-pVTZ basis sets. An explicit electronic correlation was taken into account by using the MP2/6-311+G(3df) and the high-level CCSD(T)/6-311+G* approximations. Calculated geometric parameters are listed in Table 2. All used computational methods result in very similar molecular structures. In particular, when the extended 6-311+G(3df) and aug-cc-pVTZ basis sets are used at the significantly less costly B3LYP level of approximation, the computed geometrical parameters show little dependence on the basis sets.

Conformational Space and Molecular Structure of $F_2NC(O)NCO$. The potential energy curve around the N−C single bond has been estimated by optimizing the molecular geometry every 10° for constant values of the δ[FN−C(O)] dihedral angles (Figure 3). These curves resemble those previously obtained for $F_2NC(O)F$. Moreover, similar curves are obtained for structures with mutual syn and anti orientation of the C=O with respect to the N=C bonds. Thus, the global minimum corresponds to a structure with δ[FN−C(O)] ≈ 140° and syn orientation of the carbonyl group with respect to the isocyanate group [δ(O=C−*N*=C) = 0°]. The anti conformer, with δ(O=C−N=C) = 180°, lies higher in energy by an amount of around 1 kcal/mol.

TABLE 1: Symmetry Coordinates for $F_2NC(O)F$ and $F_2NC(O)NCO$

description	symmetry coordinate	
	$F_2NC(O)F$	$F_2NC(O)NCO$
N═C═O antisymmetric stretching		$S_1 = 2^{-1/2}(E - F)$
C═O stretching	$S_1 = A$	$S_2 = A$
N═C═O symmetric stretching		$S_3 = 2^{-1/2}(E + F)$
NF_2 antisymmetric stretching	$S_2 = 2^{-1/2}(C_1 - C_2)$	$S_4 = 2^{-1/2}(C_1 - C_2)$
NF_2 symmetric stretching	$S_3 = 2^{-1/2}(C_1 + C_2)$	$S_5 = 2^{-1/2}(C_1 + C_2)$
C−N stretching	$S_4 = B$	$S_6 = B$
C−F and C−NCO stretching	$S_5 = D$	$S_7 = D$
out-of-plane C═O	$S_6 = \eta$	$S_8 = \eta$
NC(O) deformation	$S_7 = 6^{-1/2}(2\phi - \delta - \rho)$	$S_9 = 6^{-1/2}(2\phi - \delta - \rho)$
NC(O) rocking	$S_8 = 2^{-1/2}(\delta - \rho)$	$S_{10} = 2^{-1/2}(\delta - \rho)$
NF_2 twisting	$S_9 = 2^{-1/2}(\varepsilon_1 - \varepsilon_2)$	$S_{11} = 2^{-1/2}(\varepsilon_1 - \varepsilon_2)$
NF_2 wagging	$S_{10} = 2^{-1/2}(\varepsilon_1 + \varepsilon_2)$	$S_{12} = 2^{-1/2}(\varepsilon_1 + \varepsilon_2)$
NF_2 deformation (scissor)	$S_{11} = \beta$	$S_{13} = \beta$
N═C═O deformation		$S_{14} = \pi$
C−N═C deformation		$S_{15} = \lambda$
out-of-plane N═C═O		$S_{16} = \gamma$
C−NF_2 torsion	$S_{12} = \tau_1$	$S_{17} = \tau_1$
C−NCO torsion		$S_{18} = \tau_2$

TABLE 2: Computed Geometrical Parameters (distances in Å, angles in deg) for $F_2NC(O)F$ at Different Levels of Calculation

		B3LYP		
	MP2/6-311+G(3df)	6-311+G(3df)	Aug-cc-pVTZ	CCSD(T)/6-311+G*
N−F[a]	1.372	1.378	1.387	1.373
C−N	1.456	1.455	1.455	1.463
C═O	1.177	1.171	1.173	1.173
C−F	1.316	1.320	1.323	1.316
F−N−F	104.1	104.4	104.2	103.9
F−N−C[a]	106.0	107.5	107.4	106.4
N−C═O	125.8	125.6	125.9	125.8
N−C−F	107.4	107.9	107.9	107.6
F−N−C═O	134.3	139.1	139.4	134.2

[a] Averaged values.

TABLE 3: Calculated Relative Energies Corrected by Zero-Point Energy (kcal/mol) for $F_2NC(O)NCO$

	B3LYP					
	6-311+G(3df)		aug-cc-pVTZ		MP2/6-311+G(3df)	
	syn	anti	syn	anti	syn	anti
ΔE^0	0.00[a]	0.28	0.00[b]	0.35	0.00[c]	0.18

[a] $E^0 = -535.870\,564$ hartree. [b] $E^0 = -535.883\,48$ hartree. [c] $E^0 = -534.927\,898\,2$ hartree, zero-point corrections calculated at the B3LYP/6-311+G(3df) level of theory.

Additionally, full geometry optimizations and frequency calculations were accomplished for each of the stationary structures at high-levels of theoretical approximations, which include B3LYP and MP2 methods with the 6-311+G(3df) and the B3LYP/aug-cc-pVTZ levels of approximation. Predicted relative energies corrected by zero-point calculations, ΔE^0, are listed in Table 3. These calculations compute the existence of two stable forms of $F_2NC(O)NCO$, all methods agreeing with the fact that the lower energy form corresponds to the syn conformer, with the anti form being higher in energy by on the order of 0.5 kcal/mol. By taking into consideration the calculated ΔG^0 values at the B3LYP/6-311+G(3df) level of approximation ($\Delta G^0 = 0.26$ kcal/mol), a relative abundance of 39.2% of the less stable anti form is expected to be present in the vapor of $F_2NC(O)NCO$ at room temperature. The optimized molecular structures for syn and anti conformers are shown in Figure 4, and the computed geometrical parameters are given in Table 4.

TABLE 4: Computed Geometrical Parameters (distances in Å, angles in deg) for Syn and Anti Conformers of $F_2NC(O)NCO$ at Different Levels of Calculation

	B3LYP aug-cc-pVTZ		MP2 6-311+G(3df)	
parameter	syn	anti	syn	anti
N−F[a]	1.386	1.390	1.375	1.379
C−N(sp^3)	1.471	1.492	1.468	1.486
C═O	1.190	1.186	1.193	1.189
C−N(sp^2)	1.381	1.373	1.383	1.377
N═C	1.219	1.217	1.228	1.228
NC═O	1.154	1.154	1.160	1.161
F−N−F	103.8	103.3	103.7	103.3
F−N−C[a]	107.6	107.0	107.3	105.8
N−C═O	121.7	120.5	122.3	121.8
N═C═O	128.8	126.2	129.3	126.3
N−C−N	109.1	112.9	108.1	111.2
C−N═C	130.5	135.9	129.3	131.5
F−N−C═O	139.3	139.1	134.8	130.4
N−C−N═C	176.4	−10.9	176.6	−5.9

[a] Averaged values.

Vibrational Analysis. To our knowledge, no detailed vibrational studies on $NF_2C(O)F$ nor $NF_2C(O)NCO$ have been performed. Although the IR spectra were reported previously,[5,6] they have been only used as purity criteria, without any band assignments. Moreover, no reports of the Raman spectrum of difluoroaminocarbonyl compounds exist in the literature. We have expanded the previously reported data by searching both the vapor infrared and liquid phase FT-Raman spectra. Figures

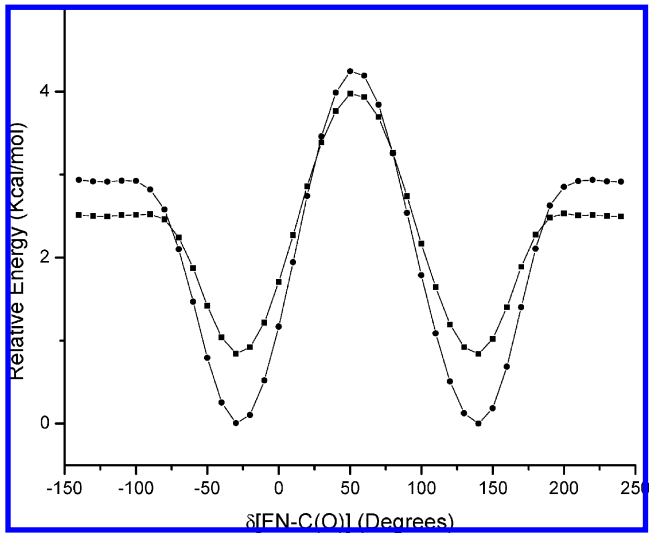

Figure 3. Calculated potential function (B3LYP/6-311+G*) for the internal rotation around the N−C bond for syn (●) and anti (■) $F_2NC(O)NCO$.

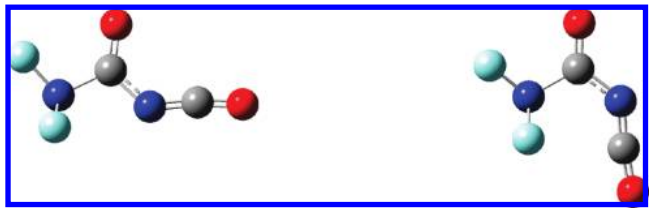

Figure 4. Molecular models for syn and anti conformers of $F_2NC(O)NCO$.

5 and 6 show the FTIR spectrum of gaseous $F_2NC(O)F$ and the FTIR and Raman spectra of gaseous and liquid $F_2NC(O)NCO$, respectively. Furthermore, frequency calculations at the B3LYP level with 6-311+G(3df) and aug-cc-pVTZ basis sets have been performed to complement the experimental results. The observed band positions in the IR and Raman spectra together with calculated wavenumbers are collected in Tables 5 and 6 for $F_2NC(O)F$ and $F_2NC(O)NCO$, respectively. The approximate description of the modes is based on the calculated displacement vectors for the fundamentals, as well as on comparison with the spectra of related molecules.[30–34] Furthermore, the PED associated with each normal vibrational mode has been calculated under the harmonic assumption. All normal modes of vibration in both $NF_2C(O)F$ and $NF_2C(O)NCO$ are active in the IR and Raman spectra in the C_1 symmetry group. From the PED analysis, it becomes clear that many vibrations have a high degree of mixture. Therefore, tentative assignments for characteristic and intense spectral features in the vibrational spectra of the molecules are discussed.

The most intense band in the IR spectrum of $NF_2C(O)F$ appears centered at 1909 cm^{-1}, showing a clear B-type contour, and can be attributed with confidence to the C═O stretching fundamental mode. The C−F stretching mode [ν(C−F)] is observed at 1211 cm^{-1} as an intense and well-structured hybrid AC-type band. The two broad bands of medium intensity centered at 1050 and 971 cm^{-1}, can be assigned to the NF_2 symmetric and antisymmetric stretching modes, respectively, in comparison with the absorptions appearing at 951 and 852 cm^{-1} and at 1029 and 904 cm^{-1} in the infrared spectra of F_2NCF_3[33] and F_2NOCF_3,[35] respectively. Two other bands of medium intensity with well-defined A and C rotational contours are observed at 838 and 769 cm^{-1} and were assigned to the

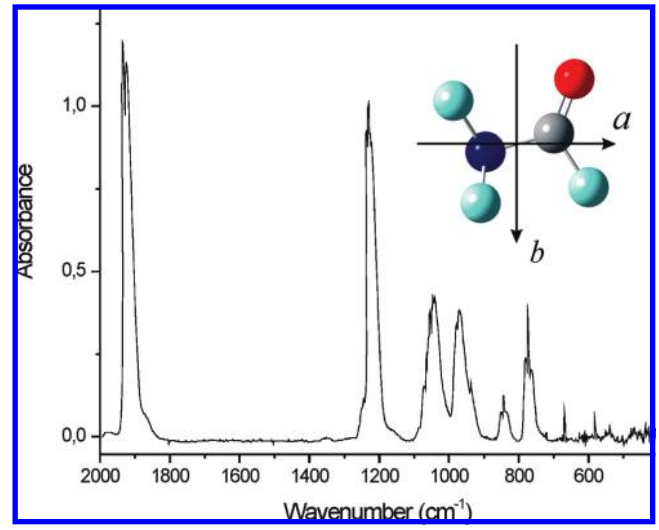

Figure 5. Gas phase FTIR at 7.0 mbar (glass cell, 200 mm optical path length, Si windows, 0.5 mm thick) for $F_2NC(O)F$. The molecular model for $F_2NC(O)F$ and main axes of inertia are also shown (the *c*-axis is perpendicular to the plane formed by the *a*- and *b*-axes).

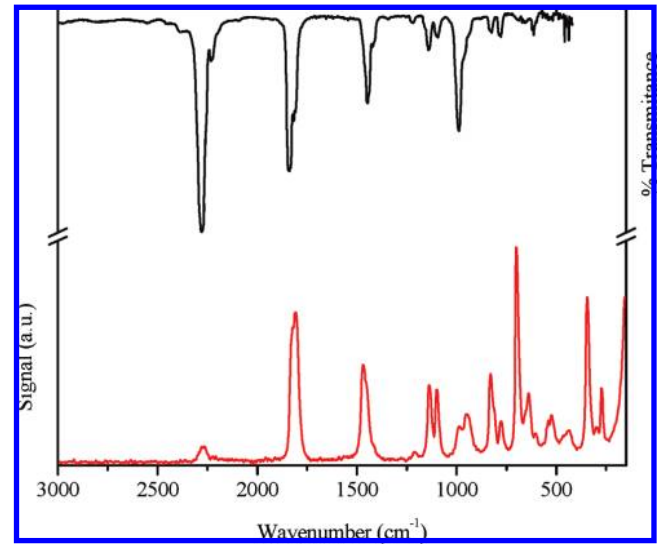

Figure 6. Gas-phase FTIR at 1.4 mbar (glass cell, 200 mm optical path length, Si windows, 0.5 mm thick) and liquid Raman spectra for $F_2NC(O)NCO$.

fundamental N−C stretching and to the out-of-plane (carbonyl) deformation modes, respectively. Their band envelopes agree with the relative orientation of the vibrating groups with respect to the principal moments of inertia (Figure 5).

For $F_2NC(O)NCO$, a strong infrared absorption in the 2280−2250 cm^{-1} region is characteristic of the isocyanate functional group.[36,37] The ν_{as}(NCO) stretching vibrational mode appears at 2277 cm^{-1} as an intense band in the gas-phase infrared spectrum with a weaker counterpart in the Raman spectrum of the liquid compound (2262 cm^{-1}). On the other hand, the corresponding symmetric motion is observed as an intense signal in the Raman spectra centered at 1458 cm^{-1}, which correlates with the medium intensity absorption observed in the infrared spectra at 1445 cm^{-1} (see Figure 6).

Two clear absorptions centered at 1836 and 1808 cm^{-1} with A and B contour, respectively, are observed in the CO stretching region of the gas-phase infrared spectrum (see Figure 7). These bands represent a signature of conformational equilibrium, as will be discussed in the next section. In the Raman spectrum

TABLE 5: Observed and Calculated Vibrational Data (cm^{-1}) for $F_2NC(O)F$

			B3LYP[a]		
IR (gas)	band contour	MP26-311+G(3df)[a]	6-311+G(3df)	aug-cc-pVTZ	tentative assignment (PED)
1914 R 1904 P	B	1938 (276)	1944 (327)	1936 (325)	ν(C=O) (100)
1217 R 1211 Q 1206 P	AC	1248 (201)	1213 (191)	1209 (195)	ν(C−F) (55) + ν(N−C) (30) + δ(NCO) (15)
1050 1036		1092 (139)	1071 (152)	1065 (147)	ν_s(N−F) (50) + ν(C−F) (25) + $\delta(NF_2)$ (10)
971 968 963 932 sh		1013 (64)	982 (88)	976 (91)	ν_{as}(N−F) (75) + ν_s(N−F) (25)
846 R 838 Q 830 P	A	858 (28)	824 (37)	821 (36)	ν(N−C) (40) + oop(C=O) (35) + δ(N−C=O) (20)
775 R 769 Q 760 P	C	787 (44)	780 (48)	777 (48)	oop(C=O) (35) + δ(C=O) (20) + ν(N−C) (20)
581		594 (5)	580 (3)	578 (3)	δ(C=O) (40) + ν(N−C) (20) + $\rho(NF_2)$ (15)
537		558 (7)	542 (7)	540 (7)	$\delta_s(NF_2)$ (50) + ρ(C=O) (20) + $\delta_{as}(NF_2)$ (15)
		485 (6)	472 (8)	470 (8)	ρ(C=O) (40) + $\delta_s(NF_2)$ (30) + δ(C=O) (20)
		341 (5)	332 (6.8)	331 (7)	$\rho(NF_2)$ (75) + oop(C=O) (20)
		280 (3)	274 (2.8)	273 (2.9)	$\delta_{as}(NF_2)$ (60) + ρ(C=O) (30)
		80 (0.8)	82 (0.7)	81 (0.7)	τ(N−C) (85)

[a] Calculated intensities are given in parentheses.

TABLE 6: Observed and Calculated Vibrational Data (cm^{-1}) for $F_2NC(O)NCO$

			B3LYP/aug-cc-pVTZ[b]		
IR (gas)[a]	band contour	Raman (liquid)	syn	anti	tentative assignment (PED)[c]
2277		2262	2338 (1295)	2342 (1191)	ν_{as}(NCO) (100)
1840 R 1836 Q 1829 P	A	1813		1861 (616)	ν(C=O) (100) (anti)
1812 R 1804 P	B	1799	1831 (363)		ν(C=O) (100) (syn)
1445 1417 sh		1458	1490 (236)	1504 (104)	ν_s(NCO) (70) + ν_{as}(C−N) (20)
1229 R 1220 P	B	1206	1157 (94)		ν_{as}(C−N) (50) + $\nu_s(NF_2)$ (25) + ν_s(NCO) (10) (syn)
1137		1131		1105 (40)	ν_{as}(C−N) (50) + $\nu_s(NF_2)$ (25) + ν_s(NCO) (10) (anti)
1094		1093	1001 (241)	1005 (264)	$\nu_s(NF_2)$ (50) + ν_s(NCO) (15) + ν_s(C−N) (10) + ν_{as}(C−N) (10)
996 R 988 Q 980 P	AC	982	965 (144)		$\nu_{as}NF_2$ (95) (syn)
955 929 sh		947		939 (62)	$\nu_{as}NF_2$ (95) (anti)
824 787 R		825	814 (93)	801 (11)	ν_s(C−N) (50) + oop(C=O) (25) + $\delta_s(F_2NC)$ (20)
780 Q 773 P	C	776	782 (47)	686 (17)	oop(C=O) (50) + ρ(C=O) (15) + $\delta_s(F_2NC)$ (10) + δ(NCO) (10)
691 R 683 P	B	691	639 (8)	658 (35)	δ(*N* = C=O) (50) + ν_s(C−N) (15) + ν_{as}(C−N) (10)
653		636	621 (22)	612 (25)	oop(NCO) (90)
611		603	552 (6)	541 (0.8)	δ(C=O) (45) + δ(NCO) (30) +$\delta(NF_2)$ (15)
551 541		521	517(13)	504 (5)	$\delta(NF_2)$ (50) + ρ(C=O) (10) + $\delta_{as}(F_2NC)$ (10)
462		434	436 (4)	468 (15)	$\delta_{as}(F_2NC)$ (40) + $\delta(NF_2)$ (20) + ρ(C=O) (10)
		338	335 (5)	340 (4)	$\delta_s(F_2NC)$ (70) + oop(C=O) (20)
		271	266 (1)	296 (7)	ρC=O (40) + $\delta_{as}(F_2NC)$ (30) + oop(NCO) (10)
			107 (0.6)	108 (0.1)	δ(C−N=C) (85) + τ(C−NCO) (10)
			87(1.2)	102 (1.5)	τ(C−NCO) (60) + τ(N−C) (30)
			61 (0.1)	40 (0.1)	τ(N−C) (90) + τ(C−NCO) (10)

[a] Tentative assignments for low-intensity nonfundamental modes: 3708 cm^{-1} [ν_{as}(N=C=O) + ν_s(N=C=O)], 3648 cm^{-1} [2 × ν(C=O)], 3361 cm^{-1} [ν_{as}(N=C=O) + $\nu_s(NF_2)$], 3263 cm^{-1} [ν(C=O) + ν_s(N=C=O)], 2926 cm^{-1} [ν(C=O) + $\nu_s(NF_2)$], 2810 cm^{-1} [2 × ν_s(N=C=O)] 2215 cm^{-1} [ν(C=O)+ $\delta_{as}(F_2NC)$]. [b] Calculated intensities are given in parentheses. [c] Unless indicated, band assignment and PED values correspond to the most stable conformer.

TABLE 7: Rotational Constants (cm^{-1}), Asymmetry Parameters,[a] and P−R Branch Separation (cm^{-1}) Calculated at the MP2/6-311+G(3df) Level for $F_2NC(O)F$ and $F_2NC(O)NCO$

										$\Delta\nu(PR)^b$	
		A	*B*	*C*	κ	ρ^*	β	$S(\beta)$	A(||)	B(⊥)	C(⊥)
$F_2NC(O)F$		0.1859	0.1237	0.0780	−0.154	0.872	0.5028	1.349	17.0	12.6	25.6
$F_2NC(O)NCO$	syn	0.1707	0.0405	0.0334	−0.896	3.389	3.212	1.192	10.3	8.6	15.5
	anti	0.1308	0.0532	0.0387	−0.685	1.732	1.460	1.272	11.0	8.6	16.4

[a] Asymmetry parameters: $\kappa = (2B - A - C)/(A - C)$, $\rho^* = (A - C)/B$, $\beta + 1 = A/B$ (prolate top), $\log S(\beta) = 0.712/(\beta + 4)^{1.13}$. [b] P−R band separation are defined and calculated according to the method of Seth-Paul.[40]

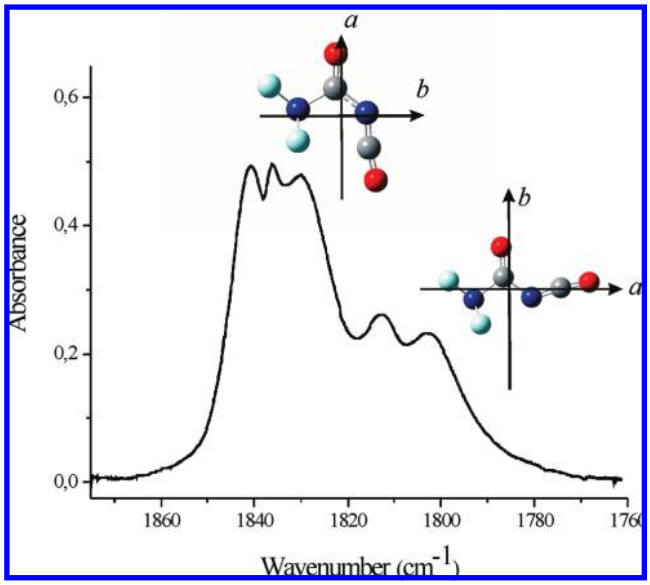

Figure 7. C═O vibrational stretching region in the IR spectrum of gaseous $F_2NC(O)NCO$ at 3.5 mbar (glass cell, 200 mm optical path length, Si windows, 0.5 mm thick). The principal axes of inertia are shown for the two rotamers in equilibrium (the *c*-axis is perpendicular to the plane formed by the *a*- and *b*-axes).

of liquid $F_2NC(O)NCO$, the carbonyl signal is observed as an intense band with two maxima at 1813 and 1799 cm^{-1}, a further indication of rotational isomerism, now in the liquid phase. The N−F stretching modes of the NF_2 group are assigned to the bands at 1094 and 988 cm^{-1} caused by the symmetric and antisymmetric group motions, respectively. For the $\nu_{as}(NF_2)$ normal mode, the calculation at the B3LYP/aug-cc-pVTZ level predicts a difference of 26 cm^{-1} between the syn and anti forms, being anti at lower frequencies. Thus, the weak absorptions at 955 cm^{-1} is tentatively assigned to the $\nu_{as}(NF_2)$ fundamental mode of the anti form. It should be noted that a similar split (982 and 947 cm^{-1}) is observed in the Raman spectrum.

Finally, two strong signals at 691 and 338 cm^{-1} are observed in the Raman spectrum of liquid $F_2NC(O)NCO$, tentatively assigned to deformation modes of the isocyanate and difluoramine moieties, respectively. For both compounds, the rest of the vibrational data is listed in Tables 5 and 6.

Vapor Contour Calculation. A detailed comparison between calculated and observed band contours in the vapor infrared spectra has been successful in establishing the main conformations of molecules.[36,38,39] The infrared spectrum of $F_2NC(O)F$ shows the presence of absorptions with well-defined band contours. Some of the bands in the spectrum of $F_2NC(O)NCO$ also show contours. Calculated rotational constants (cm^{-1}) and molecular parameters, together with estimated $\Delta\nu(PR)$ values (separation between P and R branches, in cm^{-1}) are collected in Table 7.

The symmetry parameter ($\kappa = -0.15$) calculated [MP2/6-311+G(3df)] for $NF_2C(O)F$ indicates that the molecule can be classified as a prolate asymmetrical top. The meaning of the A, B, and C band contours originated from the relative orientation of the transition dipole moments with respect to the *a*, *b*, and *c* main axis of inertia of the conformer, respectively. The separation between P- and R-branches was obtained according to Seth-Paul.[40] The results of these calculations are 17 and 26 cm^{-1} for the separation between the P- and R-branches of the A and C bands, respectively, and 13 cm^{-1} for the B-type band. As gathered in Table 5, similar separation values are observed in the gas phase spectrum of $NF_2C(O)F$, which confirm the proposed structure for the molecule.

Both forms of $F_2NC(O)NCO$ can also be classified as prolate asymmetrical top conformers, with symmetry parameter $\kappa = -0.90$ and $\kappa = -0.69$ for the syn and anti forms, respectively. The expected separation between P- and R-branches calculated for both conformers are very similar, with values of 10 and 16 cm^{-1} for A and C bands, respectively, and 9 cm^{-1} for the B band type. As expected, the predicted values for the PR separations for the two rotamers are similar (Table 7). It is important to note that structural changes should affect specific force constants for each conformer, making possible their identification in the vibrational spectra. In particular, it is well-known that the ν(C═O) normal mode of vibration is a good sensor to establish conformational properties of carbonyl-containing molecules.[36,41,42] Thus, for XC(O)NCO (X = F, Cl, CH_3O, CH_3CH_2O, and CH_3S) isocyanates, two bands were observed in the carbonyl stretching region, with well-defined rotational contours.[37,43,44] The carbonyl stretching region of the infrared spectrum of $F_2NC(O)NCO$ in the vapor phase is shown in detail in the Figure 7. Two absorptions with well-defined rotational contours become evident in this spectrum. The analysis of the band envelopment allows assigning these bands to the syn and anti forms in a straightforward manner. In effect, because the almost parallel orientation of the carbonyl oscillator with respect to the principal axis of inertia *b*, a B-type band is expected for the ν(C═O) stretching mode of the syn form. Similarly, a nearly pure A-type band is expected for the anti conformer. Indeed, as observed in Figure 7, the red-shifted C═O stretching band centered at 1808 cm^{-1} shows a B contour, whereas the second band at 1836 cm^{-1} shows a net A form. Moreover, the assignment of the absorption at higher frequencies to the C═O normal mode of vibration of the second stable anti conformer of $F_2NC(O)NCO$ is also supported by the calculations. The calculated frequency difference (B3LYP/aug-cc-pVTZ) for this mode between the two conformers is 30 cm^{-1}, in very good agreement with the experimentally observed value in the gas-phase spectrum (28 cm^{-1}). It should be stressed, however, that the band assigned to the anti form is more intense than band assigned to the more stable syn conformer. This rather astonishing behavior could be rationalized by noticing that the calculated absorption coefficient for the ν(C═O) mode in the anti form is about twice higher than that of the syn conformer

(616 and 363 km/mol, respectively at the B3LYP/aug-cc-pVTZ level of approximation, see Table 6).

The conformational composition calculated from the integrated area of both carbonyl bands in the vapor IR spectrum, taking into account the computed absorption coefficient for each mode, results in a relation of 56(5)% of the more stable syn conformer at room temperature (the estimated error limit includes uncertainties in the measured areas).

Conclusions

Conformational, structural, and vibrational properties of $F_2NC(O)F$ and $F_2NC(O)NCO$ have determined on the basis of a detailed analysis of the corresponding infrared and Raman spectra. Only one conformation belonging to the C_1 symmetry point group is expected for $F_2NC(O)F$, whereas the overall evaluation of experimental and theoretical results suggests the existence of a mixture of two conformers for $F_2NC(O)NCO$ at room temperature. From the evaluation of the infrared spectrum, the relative abundance of the most stable syn form (C═O double bond syn with respect to the N═C═O group) was estimated to be 56(5)% in the gas phase.

Acknowledgment. This paper is dedicated to Prof. Heinz Oberhammer on the occasion of his 70th anniversary. Financial support by the Volkswagen-Stiftung and the Deutsche Forschungsgemeinschaft is gratefully acknowledged. The Argentinean authors thank the ANPCYT-DAAD for the German−Argentinean cooperation Awards (PROALAR) and the DAAD Regional Program of Chemistry for Argentina. They also thank the Consejo Nacional de Investigaciones Científicas y Técnicas (CONICET), the Comisión de Investigaciones Científicas de la Provincia de Buenos Aires (CIC), República Argentina. They are indebted to the Facultad de Ciencias Exactas, Universidad Nacional de La Plata, República Argentina for financial support. M.F.E. and C.O.D.V. express their gratitude to Holger Pernice, Plácido García, Mike Finze, Stefan Balters, and Stefan von Ahsen for friendship and valuable help in the laboratory work during their stay in Duisburg.

References and Notes

(1) Ruff, O.; Giese, M. *Ber. Dtsch. Chem. Ges.* **1936**, *69B*, 684.
(2) Ruff, O.; Giese, M. *Ber. Dtsch. Chem. Ges.* **1936**, *69B*, 598.
(3) Haszeldine, R. N.; Jander, J. *J. Chem. Soc.* **1954**, 919.
(4) Fraser, G. W.; Shreeve, J. M. *Inorg. Chem.* **1965**, *4*, 1497.
(5) Fraser, G. W.; Shreeve, J. M. *Inorg. Chem.* **1967**, *6*, 1711.
(6) Wright, K. J.; Shreeve, J. n. M. *Inorg. Chem.* **1973**, *12*, 77.
(7) Shreeve, J. M.; De Marco, R. A. *Inorg. Chem.* **1971**, *10*, 911.
(8) Chapman, R. D. Organic Difluoramine Derivatives. In *Structure & Bonding*; Springer-Verlag: Berlin, 2007; Vol. 125; pp 123.
(9) Guirgis, G. A.; Phan, H.; Davis, J. F.; Durig, J. R. *J. Mol. Struct.* **1993**, *293*, 11.
(10) Durig, J. R.; Davis, J. F.; Guirgis, G. A. *J. Mol. Struct.* **1994**, *328*, 19.
(11) Della Védova, C. O.; Ulic, S. E.; Mack, H.-G.; Cutin, E. H. *J. Mol. Struct.* **1993**, *301*, 65.
(12) Durig, J. R.; Little, T. S.; Gounev, T. K.; Gardner, J. K.; Sullivan, J. F. *J. Mol. Struct.* **1996**, *375*, 83.
(13) Ulic, S. E.; Della Védova, C. O.; Aymonino, P. J. *J. Raman Spectrosc.* **1990**, *21*, 283.
(14) Mack, H.-G.; Oberhammer, H.; Della Védova, C. O. *J. Mol. Struct.* **1989**, *200*, 277.
(15) Klapstein, D.; Nau, W. M. *Spectrochim. Acta* **1994**, *50A*, 307.
(16) Mack, H.-G.; Oberhammer, H.; Della Védova, C. O. *J. Mol. Struct.* **1992**, *265*, 359.
(17) Landsberg, B. M.; Iqbal, K. *J. Chem. Sc., Faraday Trans. 2* **1980**, *76*, 1208.
(18) Njuyen, M. T.; Hajnal, M. R.; Vanquickenborne, L. G. *J. Mol. Struct.* **1991**, *231*, 185.
(19) Mack, H.-G.; Oberhammer, H. *J. Mol. Struct. (THEOCHEM)* **1992**, *258*, 197.
(20) Jonas, V.; Frenking, G. *Chem. Phys. Lett.* **1991**, *177*, 175.
(21) Balfour, W. J.; Fougère, S. G.; Klapstein, D.; Nau, W. M. *J. Mol. Struct.* **1993**, *299*, 21.
(22) Badawi, H. M.; Förner, W. *Spectrochim. Acta A* **2003**, *A59*, 335.
(23) Badawi, H. M.; Förner, W.; Abu-Sharkh, B. F.; Oloriegbe, Y. S. *J. Mol. Mod.* **2002**, *8*, 44.
(24) Zeng, X.-Q.; Yao, L.; Ge, M.-F.; Wang, D.-X. *J. Mol. Struct.* **2006**, *789*, 92.
(25) Ge, M.; Ma, C.; Xue, W. *J. Phys. Chem. A* **2009**, *113*, 3108.
(26) Gombler, W.; Willner, H. *J. Phys. E* **1987**, *20*, 1286.
(27) Frisch, M. J.; Trucks, G. W.; Schlegel, H. B.; Scuseria, G. E.; Robb, M. A.; Cheeseman, J. R.; Montgomery, J. A., Jr.; Vreven, T.; Kudin, K. N.; Burant, J. C.; Millam, J. M.; Iyengar, S. S.; Tomasi, J.; Barone, V.; Mennucci, B.; Cossi, M.; Scalmani, G.; Rega, N.; Petersson, G. A.; Nakatsuji, H.; Hada, M.; Ehara, M.; Toyota, K.; Fukuda, R.; Hasegawa, J.; Ishida, M.; Nakajima, T.; Honda, Y.; Kitao, O.; Nakai, H.; Klene, M.; Li, X.; Knox, J. E.; Hratchian, H. P.; Cross, J. B.; Adamo, C.; Jaramillo, J.; Gomperts, R.; Stratmann, R. E.; Yazyev, O.; Austin, A. J.; Cammi, R.; Pomelli, C.; Ochterski, J. W.; Ayala, P. Y.; Morokuma, K.; Voth, G. A.; Salvador, P.; Dannenberg, J. J.; Zakrzewski, V. G.; Dapprich, S.; Daniels, A. D.; Strain, M. C.; Farkas, O.; Malick, D. K.; Rabuck, A. D.; Raghavachari, K.; Foresman, J. B.; Ortiz, J. V.; Cui, Q.; Baboul, A. G.; Clifford, S.; Cioslowski, J.; Stefanov, B. B.; Liu, G.; Liashenko, A.; Piskorz, P.; Komaromi, I.; Martin, R. L.; Fox, D. J.; Keith, T.; Al-Laham, M. A.; Peng, C. Y.; Nanayakkara, A.; Challacombe, M.; Gill, P. M. W.; Johnson, B.; Chen, W.; Wong, M. W.; Gonzalez, C.; Pople, J. A. *Gaussian 03*, Revision B.04 ed.; Gaussian, Inc.: Pittsburgh PA, 2003.
(28) Scheiner, A. C.; Baker, J.; Andzelm, J. W. *J. Comput. Chem.* **1997**, *18*, 775.
(29) Hedberg, L.; Mills, I. M. *J. Mol. Spectrosc.* **2000**, *203*, 82.
(30) Fox, W. B.; Anderson, L. R. *Inorg. Chem.* **1968**, *7*, 382.
(31) Shreeve, J. M.; Duncan, L. C.; Cady, G. H. *Inorg. Chem.* **1965**, *4*, 1516.
(32) Erben, M. F.; Della Védova, C. O.; Willner, H. *J. Mol. Struct.* **2004**, *692*, 63.
(33) Oberhammer, H.; Günter, H.; Burger, H.; Heyder, F.; Pawelke, G. *J. Phys. Chem.* **1982**, *86*, 664.
(34) Erben, M. F.; Pis Diez, R.; Della Védova, C. O. *Chem. Phys.* **2005**, *308*, 193.
(35) Maya, W.; Pilipovich, D.; Warner, M. G.; Wilson, R. D.; Christe, K. O. *Inorg. Chem.* **1983**, *22*, 810.
(36) Campbell, N. L.; Gillis, C. J.; Klapstein, D.; Nau, W. M.; Balfour, W. J.; Fougère, S. G. *Spectrochim. Acta* **1995**, *51A*, 787.
(37) Balfour, W. J.; Fougère, S. G.; Klapstein, D.; Nau, W. M. *Can. J. Chem.* **1993**, *71*, 1627.
(38) Álvarez, R. M. S.; Cutín, E. H.; Romano, R. M.; Mack, H. G.; Della Védova, C. O. *Spectrochim. Acta* **1998**, *A54*, 605.
(39) Argüello, G. A.; Jüelicher, B.; Ulic, S. E.; Willner, H.; Casper, B.; Mack, H.-G.; Oberhammer, H. *Inorg. Chem.* **1995**, *34*, 2089.
(40) Seth-Paul, W. A. *J. Mol. Struct.* **1969**, *3*, 403.
(41) Erben, M. F.; Della Védova, C. O.; Romano, R. M.; Boese, R.; Oberhammer, H.; Willner, H.; Sala, O. *Inorg. Chem.* **2002**, *41*, 1064.
(42) Erben, M. F.; Della Védova, C. O.; Boese, R.; Willner, H.; Oberhammer, H. *J. Phys. Chem. A* **2004**, *108*, 699.
(43) Torrico Vallejos, S.; Erben, M. F.; Willner, H.; Boese, R.; Della Védova, C. O. *J. Org. Chem.* **2007**, *72*, 9074.
(44) Klapstein, D.; Nau, W. M. *J. Mol. Struct.* **1993**, *299*, 29.

JP907827Q